Apparent and Average Acceleration of the Universe

William Frost

October 2, 2010

Abstract

We study two forms of deceleration parameter, one derived from supernova observations and the other from the Buchert averaging scheme. This work followed the analysis of Bolejko and Andersson in their paper "Apparent and Average Acceleration of the Universe". We have recalculated the volume deceleration parameter, q^{vol}, and the distance deceleration parameter, q^{dis}, within Lemaître-Tolman models. Within the models studied, those which are realistic and fit supernova data are found to have $q^{vol} > 0$, while those which Bolejko and Andersson found with $q^{vol} < 0$ were deemed unrealistic. Mistakes in their paper were found and corrected. The deceleration parameter was found not to be directly related to the volume deceleration parameter.

Contents

Chapter 1

Introduction

Homogeneous Models

Friedmann models were first analysed by Alexander Friedmann in 1922 and 1924 [1] [2]. Other famous names have been branded onto these models such as Georges Lemaître, Howard Percy Robertson and Arthur Geoffrey Walker. The metric associated with this model is often referred to as the Friedmann-Lemaître-Robertson-Walker (FLRW) metric. These models assume homogeneity and isotropy; two assumptions which are philosophical ideals, something not mirrored on all scales by the Universe. This gives us a comparatively simple solution to Einstein's equations in terms of a featureless *perfect fluid*. With such simplifications it is surprising that the current Concordance model of the Universe is a modified Friedmann model, know as the Lambda Cold Dark Matter (ΛCDM) model. ΛCDM is a Friedmann model with parameters specific to observations of WMAP and supernova data [3] [4] [1], and is very successful at explaining many observations including the expansion and age of the Universe, abundance of light elements, present mass density [5](pp. 9-11). But this simplistic model does not come without a price – supernova type 1a (SN1a) data gives luminosities which appear too weak to fit an unmodified Friedmann model, so a certain breed of cosmologists have added the *cosmological constant* (the Λ in ΛCDM) to 'fix' this problem. This seemingly simple addition of a constant introduces physical implications which are known today as one of the greatest problems in modern physics, there is currently no theoretical understanding of the origin or magnitude of the cosmological constant [6].

Structure, however, is observed in the Universe, in the form of walls, filaments and voids [7]. Given this structure, we should question the validity of a perfect featureless fluid Universe and the model that describes it. It is noted that Friedmann models also suffer from the *coincidence problem* [8]: they do not explain why the acceleration has started in the recent past. The most significant change of late, is the formation of large-scale structure and so the recent acceleration may be related to the growth of inhomogeneity.

[1] See [3] for the latest supernova data and [4] for discussion of the latest WMAP data

Inhomogeneous Models

One of the main reasons for using homogeneous models is because of the great simplification to Einstein's equations; removing the symmetries of homogeneity and isotropy greatly increases complexity – due to the non-linearity of Einstein's equations. There are many approaches to inhomogeneity in the literature; the three main approaches are: exact solutions, averaging solutions and perturbative solutions. Here we choose to focus on the first two.

Exact solutions of Einstein's equations are very difficult to find. Most of those that have been found are highly symmetric – an example is the Lemaître-Tolman model which has spherical symmetry. Alternatively we have the averaging approach. The idea here is to determine the average evolution of the universe by a suitable average of an evolving inhomogeneous geometry and matter distribution. One much used approach is to average scalar quantities such as density, expansion and scalar curvature over spatial hypersurfaces which correspond to the constant time of the rest frame of the cosmic dust. Using a simple volume average, we arrive at the Buchert equations [9]. These equations are very similar to the Friedmann equations, differing by a term called *backreaction*. The existence of backreaction means that the Friedmann model using averaged inhomogeneous data is missing information and therefore will not give the correct evolution expected by Einstein's general theory of relativity.

Using the Buchert equations, many authors [10, 11, 12, 13] have shown that a negative volume deceleration parameter, q^{vol}, can be found. That is, the volume over which quantities are averaged in the models studied, increases in an accelerated fashion with time. However, it is not obvious how this parameter relates to the deceleration parameter "measured" by SN1a observations, q^{dis}, if at all. So a question remains – is there a relationship between these two parameters; i.e., does $q^{vol} < 0 \implies q^{dis} < 0$?

This project compares the two deceleration parameters within the limits of the Lemaître-Tolman model, following the analysis of Bolejko and Andersson [14]. The reason for choosing the Lemaître-Tolman model is that it can be solved exactly and the two parameters can be compared easily. My explicit contribution was through reproducing, and correcting, some of the results of the paper.

Chapter 2

Averaging Procedure

We wish to average quantities in a region of spatial hypersurfaces with an appropriately chosen parameter of constant cosmological time. To do this we look at a $(3+1)$ split of Einstein's equations, in the absence of the cosmological constant, and a simple average across these spatial hypersurfaces. We follow the derivation due to Buchert [9].

(3+1) decomposition of Einstein's equations

In general relativity spacetime curvature is determined by the occurence of the Riemann tensor in the equation of geodesic deviation. The Reimann tensor may be decomposed into pieces $\sigma_{\mu\nu}$, θ, $\omega_{\mu\nu}$, which represent the shearing, expansion, and rotation of a congruence of geodesics. We restrict ourselves to an irrotational fluid, rotation tensor $\omega_{\mu\nu} = 0$, with the simplest matter model 'dust', pressure free, $p = 0$. We can construct hypersurfaces that are orthogonal to the flow of our comoving 'dust', whose four-velocity we denote by u^μ, such that $u^\mu u_\mu = -c^2$. This is the 3+1 ADM space-time foliation with a constant lapse time and vanishing shift vector. For further reading on the ADM formalism the reader is directed to [15].

The energy-momentum tensor for such a fluid is $T_{\mu\nu} = \rho u_\mu u_\nu$ [16] (pp. 34). Without the introduction of *dark energy* through the cosmological constant Einstein's equations are:

$$G_{\mu\nu} = \kappa T_{\mu\nu} \tag{2.1}$$

$$\implies \mathcal{R}_{\mu\nu} - \frac{1}{2} g_{\mu\nu}\mathcal{R} = \kappa\rho u_\mu u_\nu \tag{2.2}$$

with Ricci Tensor $\mathcal{R}_{\mu\nu}$, Ricci scalar $\mathcal{R}$ (trace of Ricci tensor), ρ the rest density. We have conservation of local energy expressed through the equation

$$(\rho u^\mu u^\nu)_{;\mu} = 0 \tag{2.3}$$

The spatial hypersurfaces are described by the projection tensor, $P_{\alpha\beta} = g_{\alpha\beta} + u_\alpha u_\beta$, which projects indexed quantities onto the hypersurface via contraction. For the remainder of this section Gaussian coordinates are used, which are coordinates comoving with the fluid. It is noted that these coordinates are equivalent to lagrangian coordinates in fluid mechanics, showing the strong mathematical link between general relativity and fluid mechanics.

The 'interval' or 'length element' becomes:

$$ds^2 = -c^2dt^2 + g_{ij}dx^i dx^j \tag{2.4}$$

with the spatial 3-metric $g_{ij} = h_{ij}$. The rate of change of the projection tensor in the normal vector field (here the dust four-velocity) direction gives a measure of the curvature of the hypersurface and is known as the extrinsic curvature tensor, $K_{\mu\nu}$ defined by [16] (Appendix D, equation (D.43)):

$$K_{\mu\nu} \equiv -\frac{1}{2}\mathcal{L}_u P_{\mu\nu} \implies K_{ij} = -P^{\alpha}{}_{i}P^{\beta}{}_{j}u_{\beta;\alpha} \tag{2.5}$$

Note that there are two common conventions used for $K_{\mu\nu}$; that given above and also minus this value. For example, Buchert [9] uses the above convention whereas Carroll [16] (Appendix D) uses the other.

In this $(3+1)$ split, Einstein's equations and the continuity equation (2.3) are equivalent to [17]

$$\begin{aligned}
\frac{1}{2}\left(\mathcal{R} + K^2 - K^i{}_j K^j{}_i\right) &= \kappa\rho, &(2.6)\\
K^i{}_{j||i} - K_{|j} &= 0, &(2.7)\\
\dot{\rho} &= K\rho, &(2.8)\\
(g_{ij})^{\cdot} &= -2g_{ik}K^k{}_j, &(2.9)\\
(K^i{}_j)^{\cdot} &= KK^i{}_j + \mathcal{R}^i{}_j - \frac{\kappa}{2}\delta^i{}_j, &(2.10)
\end{aligned}$$

where $\mathcal{R} = \mathcal{R}^i{}_i$, $K = K^i{}_i$ and $^{\cdot} \equiv \frac{\partial}{\partial t}$. From the definition of K_{ij} and considerations of geodesic congruences for an *irrotational* fluid, we can split the extrinsic curvature tensor in terms of the expansion scalar, θ, and the shear tensor, σ_{ij} (see [16] - Appendix F for further discussion):

$$-K_{ij} = \Theta_{ij} = \frac{1}{3}\theta g_{ij} + \sigma_{ij}, \tag{2.11}$$

the trace of which is $-K = \theta$ where $\theta = \Theta^i{}_i$.

Equations (2.6) to (2.10) in this order can then be rewritten in terms of the kinematical parameters in (2.11) as:

$$\begin{aligned}
\frac{1}{2}\mathcal{R} + \frac{1}{3}\theta - \sigma^2 &= \kappa\rho, &(2.12)\\
\sigma^i{}_{j||i} &= \frac{2}{3}\theta_{ij}, &(2.13)\\
\dot{\rho} &= \theta\rho, &(2.14)\\
(g_{ij})^{\cdot} &= \frac{2}{3}g_{ij}\theta + 2\sigma_{ij}, &(2.15)\\
(\sigma^i_j)^{\cdot} &= \frac{2}{3}\delta^i{}_j\left(\kappa\rho + \sigma^2 - \frac{1}{3}\theta^2\right) - \theta\sigma^i{}_j - \mathcal{R}^i{}_j. &(2.16)
\end{aligned}$$

Where we have introduced the shear scalar $\sigma^2 = \frac{1}{2}\sigma^i{}_j\sigma^j{}_i$. Contracting (2.10) on i, j and using (2.12) we can derive *Raychaudhuri's equation*:

$$\dot{\theta} + \frac{1}{3}\theta^2 + 2\sigma^2 + \frac{1}{2}\kappa\rho = 0. \tag{2.17}$$

Denoting $J = \sqrt{\det(g_{ij})}$ and using the mathematical identity $\ln(\det(g_{ij})) = \mathrm{Tr}(\ln(g_{ij}))$ with (2.8) we obtain the identity:

$$\dot{J} = -KJ = \theta J \tag{2.18}$$

Finally, using this identity on equation (2.14) gives us the rest mass density as a function of time:

$$\rho(t, x^i) = \left(\rho(t_0, x^i)J(t_0, x^i)\right) J(t, x^i)^{-1} \tag{2.19}$$

Buchert Scheme

In the Buchert scheme, spatially averaging of a scalar field Ψ as a function of the coordinates and time on an arbitrary compact portion of the fluid D is defined by the volume integral

$$\langle\Psi(t, x^i)\rangle_D \equiv \frac{1}{V_D}\int_D Jd^3x\Psi(t, x^i) \tag{2.20}$$

$$V_D(t) \equiv \int_D Jd^3x, \tag{2.21}$$

with volume element $dV \equiv Jd^3x$ (J as defined above) on the spatial hypersurfaces of constant time and the volume V_D of the given domain D.

Analogously to the Friedmann model we can introduce an *'effective scale factor'* $a_D(t)$ specific to each domain D, given by

$$a_D(t) = \frac{V_D(t)}{V_D(t_0)} \tag{2.22}$$

where t_0 is the value of cosmic time at present, thus $V_D(t_0)$ is the initial volume. We can write the averaged expansion scalar in terms of our 'effective scale factor':

$$\langle\theta\rangle_D = 3\frac{\dot{a}_D(t)}{a_D(t)} \tag{2.23}$$

which follows from (2.18) and (2.22).

The total rest mass of our 'dust fluid' within domain D is given by:

$$M_D = \int_D Jd^3x\rho = constant, \tag{2.24}$$

with this constancy following from equation (2.19) and we have substituted $V_D(t) = V_D(t_0)a_D(t)^3$. Thus we find the total rest mass within our domain remains constant; our domain moves

with the matter.

Now we prove an important lemma for an arbitrary scalar field Ψ:

Lemma (Commutation Rule):

$$\frac{\partial}{\partial t}\langle\Psi\rangle_D - \langle\frac{\partial\Psi}{\partial t}\rangle_D = \langle\Psi\theta\rangle_D - \langle\Psi\rangle\langle\theta\rangle_D \tag{2.25}$$

Proof:

$$\begin{aligned}
\frac{\partial}{\partial t}\langle\Psi\rangle_D - \langle\frac{\partial\Psi}{\partial t}\rangle_D &= \frac{\partial}{\partial t}\left(\frac{1}{V_D(t)}\int_D Jd^3x\Psi\right) - \frac{1}{V_D(t)}\int_D Jd^3x\frac{\partial\Psi}{\partial t} \\
&= \frac{1}{V_D(t)}\frac{\partial}{\partial t}\int_D Jd^3x\Psi - \frac{1}{V_D(t)^2}\frac{\partial V_D(t)}{\partial t}\int_D Jd^3x\Psi - \frac{1}{V_D(t)}\int_D Jd^3x\frac{\partial\Psi}{\partial t} \\
&= \frac{1}{V_D(t)}\int_D \dot{J}d^3x\Psi - \frac{\dot{V}_D(t)}{V_D(t)}\frac{1}{V_D(t)}\int_D Jd^3x\Psi \\
&= \frac{1}{V_D(t)}\int_D \theta Jd^3x\Psi - \frac{\dot{V}_D(t)}{V_D(t)}\frac{1}{V_D(t)}\int_D Jd^3x\Psi
\end{aligned}$$

where the last line comes from equation (2.18), giving the required result. This lemma is of great importance; it tells us that evolution of an averaged Universe is in general different from averaging the evolved Universe. Equation (2.25) translates to: "evolution after averaging is not the same as averaging after evolving". When we use the Friedmann model, we are effectively evolving after averaging, when what we really should be doing is averaging after evolving if we want the true evolution of the Universe under Einstein's gravity. See [18] for an interesting discussion of backreaction within the Lemaître-Tolman model.

We now have all the required equations to derive the Buchert equations. An average over D on our spatial hypersurface for equations (2.12) and (2.17) yields:

$$3\left(\frac{\dot{a}_D}{a_D}\right)^2 = \kappa\langle\rho\rangle_D - \frac{1}{2}\langle R\rangle_D - \frac{\mathcal{Q}_D}{2} \tag{2.26}$$

$$3\left(\frac{\ddot{a}_D}{a_D}\right) = -\frac{1}{2}\kappa\langle\rho\rangle_D + \mathcal{Q}_D \tag{2.27}$$

with $\langle\rho\rangle_D = \frac{M_D}{V_D(t_0)a_D^3} = \frac{M_D}{V_D}$ the averaged rest mass density and $\mathcal{Q}_D = \frac{2}{3}\left(\langle\theta^2\rangle - \langle\theta\rangle^2\right) - 2\langle\sigma^2\rangle$, is known as 'backreaction'. Backreaction is the difference between the Buchert equations and the Friedmann equations, where it is neglected.

As they stand, these equations do not form a closed system of differential equations. From (2.26) and (2.27) we can derive the integrability condition:

$$\frac{\partial}{\partial t}\left(a_D^6\mathcal{Q}_D\right) + a_D\frac{\partial}{\partial t}\left(a_D^2\langle\mathcal{R}\rangle_D\right) = 0, \tag{2.28}$$

which we require to hold for a solution to exist.

Chapter 3

The Lemaître-Tolman model

The exact, spherically symmetric, irrotational and pressure free solution to Einstein's equations was discovered by Lemaître in 1933 [19]. This solution is known by many names due to efforts of other people [20, 21], but I will refer to it as the Lemaître-Tolman solution. The Lemaître-Tolman metric can be found by symmetry arguments. Requiring irrotational dust and a spherically symmetric distribution gives us the metric:

$$ds^2 = -c^2dt^2 + \frac{\left[R'(r,t)\right]^2}{1+2E(r)}dr^2 + R^2(r,t)\left[d\theta^2 + \sin^2\theta d\phi^2\right] \tag{3.1}$$

where a prime, $'$, denotes $\frac{\partial}{\partial r}$. The metric is given in a comoving coordinate system for radially moving dust particles: i.e., the *cosmic time* parameter, t, is the proper time of particles at fixed spatial coordinates, r, θ, ϕ. The motion of such particles is described via the time dependence of $R(r,t)$. The function $E(r)$ is an integration function which in the special case of a spherical symmetric vacuum solution – the Schwarzschild geometry – represents the kinetic energy per unit rest mass of particles in a congruence of radial geodesics. In the non-vacuum L-T models it still is related to the particle energies and is analogous to the Gaussian curvature k of the Friedmann models, the two being related by $E = -\frac{1}{2}kc^2$. We are using the Lorentz signature $(-,+,+,+)$; putting a restriction on $E(r)$ such that $E(r) > -\frac{1}{2}$. For this model, Einstein's equations are then equivalent to:

$$\dot{R}^2(r,t) = \frac{2M(r)}{R(r,t)} + 2E(r) \tag{3.2}$$

$$\kappa\rho(r,t)c^2 = \frac{2M'(r)}{R'(r,t)R^2(r,t)} \tag{3.3}$$

where $M(r)$ is another integration constant dependent on boundary conditions and $\kappa = \frac{8\pi G}{c^4}$.

Equation (3.2) can be solved by simple integration to yield:

$$\int_0^R \frac{d\tilde{R}}{\sqrt{2E + \frac{2M}{\tilde{R}}}} = c\left[t - t_B(r)\right]. \tag{3.4}$$

As we will see in Chapter 5, this equation can be used to calculate $E(r)$ for a given model. The function $t_B(r)$ is the *bang time* - the time of the big bang - which in Friedmann models

is independent of position, but as we see here, is a function of radial coordinate. This is due to the introduction of spherically symmetric inhomogeneities.

The expansion scalar θ, shear scalar σ and spatial Ricci scalar $\mathcal{R}$ can be found to be (see for example: [22], [23]):

$$\theta(r,t) = 2\frac{\dot{R}(r,t)}{R(r,t)} + \frac{\dot{R}'(r,t)}{R'(r,t)} \tag{3.5}$$

$$\sigma(r,t)^2 = \frac{1}{3}\left(\frac{\dot{R}(r,t)}{R(r,t)} - \frac{\dot{R}'(r,t)}{R'(r,t)}\right)^2 \tag{3.6}$$

$$\mathcal{R}(r,t) = \frac{-4}{R^2(r,t)R'(r,t)}\frac{\partial}{\partial r}(R(r,t)E(r)) \tag{3.7}$$

To find a unique solution for the L-T model we require two initial functions and a choice of gauge – in general we choose $R(r,t_0) = r$ where t_0 is the current cosmic time (reference?). This can be a specification of $E(r)$ and $M(r)$, or as in some of the models given in [14] $\rho(r)$ and $t_B(r)$ – they just need to be independent conditions. Another example is shown in [24], where an initial and final density is specified.

A further parameterisation can also be of use for modeling. Mattsson's [25] parameterisation, which can be useful for some models in the calculations of chapter 5, defines $H_0(r)$ and $\Omega(r)$ by

$$M(r) = \frac{1}{2}H_0(r)^2\Omega(r)R_0(r)^3 \tag{3.8}$$

$$E(r) = \frac{1}{2}H_0(r)^2(1-\Omega(r))R_0(r)^2 \tag{3.9}$$

where $R_0(r) \equiv R(r,t_0)$ and from which it follows:

$$H(r,t)^2 = H_0(r)^2\left[\Omega(r)\left(\frac{R_0(r)}{R(r,t)}\right)^3 - (\Omega(r)-1)\left(\frac{R_0(r)}{R(r,t)}\right)^2\right]. \tag{3.10}$$

It becomes evident that with this parametrisation $H(r,t_0) = H_0(r)$.

Chapter 4

The Apparent and Average Acceleration

Within the Friedmann model the deceleration parameter is defined as

$$q = -\frac{\ddot{a}a}{\dot{a}^2}. \tag{4.1}$$

This shows that for a Friedmann model with scale factor a, q is a measure of how the rate of expansion of the volume of the Universe decreases with time. Since the Buchert scheme admits a set of equations very similar to the Friedmann equations we can analogously define a volume deceleration parameter with use of equations (2.26) and (2.27)

$$q^{vol} = -\frac{\ddot{a_D}a_D}{\dot{a_D}^2} = -\frac{-\frac{1}{2}\kappa\langle\rho\rangle_D + \mathcal{Q}_\mathcal{D}}{\kappa\langle\rho\rangle_D - \langle\mathcal{R}\rangle_D - \frac{1}{2}\mathcal{Q}_D}, \tag{4.2}$$

so called because it is directly related to the deceleration of the volume as in the Friedmann model.

We can also introduce a deceleration parameter relating to distances. Within the Friedmann model the deceleration parameter (4.1) is identical the parameter in the following Taylor series expansion of the luminosity distance with respect to redshift:

$$\begin{aligned} D_L &= D_L|_{z=0} + \frac{dD_L}{dz}\Big|_{z=0} z + \frac{1}{2}\frac{d^2D_L}{dz^2}\Big|_{z=0} z^2 + \mathcal{O}(z^3) && (4.3)\\ &= \frac{c}{H_0}z + \frac{c}{2H_0}(1-q)z^2 + \mathcal{O}(z^3). && (4.4) \end{aligned}$$

Equation (4.3) can be applied to the Lemaître-Tolman model with use of the equation $D_L(z) = (1+z)^2 D_A(z)$, where $D_A(z)$ is known as the angular distance, which was proved as a general equation by Etherington in 1933 [**?**]. In the Lemaître-Tolman model the interval gives $D_A(z) = R(r(z), t(z))$ and so $D_L(z) = (1+z)^2 R(r(z), t(z))$, thus we have:

$$\begin{aligned} \frac{dD_L}{dz} &= 2R + \dot{R}\frac{dt}{dz} + R'\frac{dr}{dz} && (4.5)\\ \frac{d^2D_L}{dz^2} &= 2R + 4\dot{R}\frac{dt}{dz} + 4R'\frac{dr}{dz} + \ddot{R}\left(\frac{dt}{dz}\right)^2 + 2\dot{R}'\frac{dt}{dz}\frac{dr}{dz} + R''\left(\frac{dr}{dz}\right)^2 + \dot{R}\frac{d^2t}{dz^2} + R'\frac{d^2r}{dz^2} && (4.6) \end{aligned}$$

where $\frac{dt}{dz}$ and $\frac{dr}{dz}$ can be found via considerations of null geodesics passing through the origin [25]:

$$\frac{dt}{dz} = -\frac{R'(r,t)}{(1+z)\dot{R}'(r,t)}, \qquad \frac{dr}{dz} = \frac{c\sqrt{1+2E(r)}}{(1+z)\dot{R}'(r,t)}. \tag{4.7}$$

Which yields

$$H_0^{dis} = \frac{\dot{R}'}{R'}, \qquad q_0^{dis} = -\frac{R'\ddot{R}}{\dot{R}'^2} - \frac{cR''}{R'\dot{R}'} + \frac{c\dot{R}''}{\dot{R}'^2} \qquad r = 0 \tag{4.8}$$

$$H^{dis} = c\left(\frac{dD_L}{dz}\right)^{-1}, \qquad q^{dis} = 1 - \frac{H^{dis}}{c}\frac{d^2D_L}{dz^2} \qquad \forall r \geq 0 \tag{4.9}$$

Under the assumption that the Universe is a Lemaître-Tolman toy model, the distance deceleration parameter is of much use. Given supernova data in our model Universe, we can plot D_L as a function of z and find q^{dis}. Thus when considering a model, a good test is to see if its calculated q^{dis}, by equations above, matches what is 'observed'.

Apparent Acceleration

It is noted that $q^{dis} = q = -\frac{\ddot{a}a}{\dot{a}^2} = q^{vol}$ in the Friedmann model, and this is why observations giving $q^{dis} < 0$ are said to show an accelerated expansion of the Universe. However, if the model is *not* Friedmannian, then we do not in general have q^{dis} representative of deceleration and so this parameter cannot tell us directly if the Universe is accelerating. If the Friedmann model is not the correct model to describe the Universe then it could be that the accelerated expansion is only apparent – due to our model bias.

In the Lemaître-Tolman model a measure of the decelerated expansion can be found using the average parameter q^{vol}. There is then a question as to whether or not we can relate q^{vol} to the 'observable' q^{dis} in the hope that observations can tell us the acceleration of the Universe. This will be analysed in some model examples which follow. Using the 'simple' Lemaître-Tolman toy model may give us insight as to whether this can be done in general.

Chapter 5

Examples and Discussion

Models 1-4

Bolejko and Andersson [14], have examined four models which fit the SN1a data of the Riess gold sample [26], with fits just as good as the ΛCDM model according to χ^2 tests. For a plot of the residual Hubble diagram see figure 1 in [14]. Here, the models have been reanalysed and the distance deceleration parameter and volume deceleration parameter plotted in figures (5.1a) and (5.1b). The distance deceleration parameter, q^{dis}, was calculated using equation (4.9) with $\frac{dt}{dz}$ and $\frac{dr}{dz}$ from equations (4.7) along null geodesics. *(This is the part that hasn't been done properly yet - still errors)*

We note that the plots of q^{dis} vary in sign with R – each model beginning positive and dropping off to negative values within the first 0.1 Gpc. This is in contrast to the plots of q^{vol}, which are positive for all R. Thus, contrary to the Friedmann model in which $q^{vol} < 0$ requires $q^{dis} < 0$ because $q^{vol}_{friedmann} = q^{dis}_{friedmann}$, the ability of a model to reproduce SN1a data does not require $q^{vol} < 0$, i.e., the averaged Universe need not be accelerating. The volume deceleration parameter, q^{vol}, was calculated using equation (4.2).

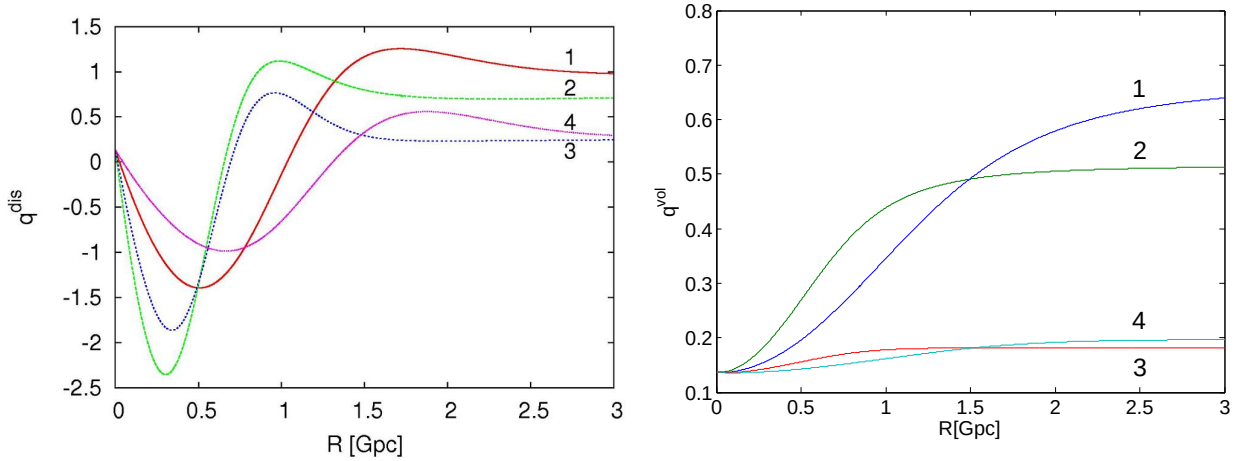

(a) Distance deceleration parameter

(b) The volume deceleration parameter

Figure 5.1: Models 1-4 distance and volume deceleration

Bolejko and Andersson went on to look at 'realistic' cosmic structures; Galaxy clusters, voids and superclusters. There are many known cosmic structure models in which $\Lambda = 0$ but $q^{vol} < 0$; the following models were studied to see if there are realistic evolving models which have $q^{vol} < 0$.

Models 5a and 5b

Model 5 is the Nevarro-Frenk-White (NFW) density distribution which was proposed by Nevarro, Frenk and White [27] as a model of Cold Dark Matter halos. It is described by the density distribution $\frac{\rho(r)}{\rho_{crit}} = \frac{\delta}{(\frac{r}{r_s})(1+\frac{r}{r_s})^2}$. It is an empirical relation which is not valid as $r \to 0$. Here it is used only for illustrative purposes, showing how changing $E(r)$ changes q^{vol} and its physical implications. This distribution has a singularity at the origin, so we modify it by matching the profile to a non-singular function near the origin. For more details see appendix A.

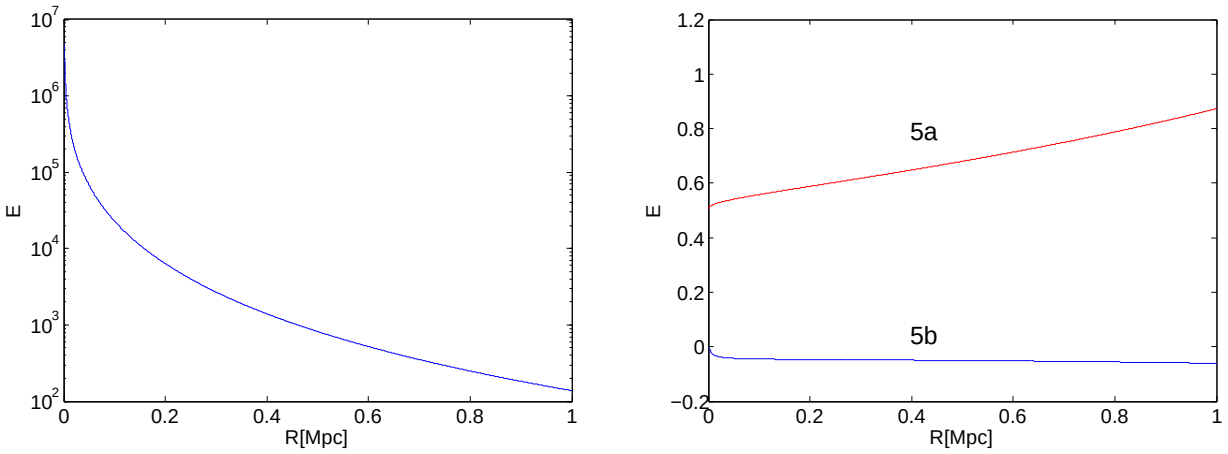

(a) The current density profile

(b) The volume deceleration parameter

Figure 5.2: Models 5a and 5b - NFW distribution

In figure (5.2*b*) q^{vol} for two models with the same NFW density profile have been plotted, the density profile is plotted in figure (5.2*a*). Figures (5.3*a*) and (5.3*b*) plot $E(r)$ for each model. The bang time is effected by this choice of E; for model 5*a* $t_B \approx$ ..? and for model 5*b* $t_B \approx$ ...?.

So while this model is not at all likely to explain any observational data for our Universe, it shows us that making E large can yield a negative volume deceleration parameter, but also an unrealistic age of the Universe as $t_B \approx$ ... puts the age of the model Universe at a few hundred thousand years.

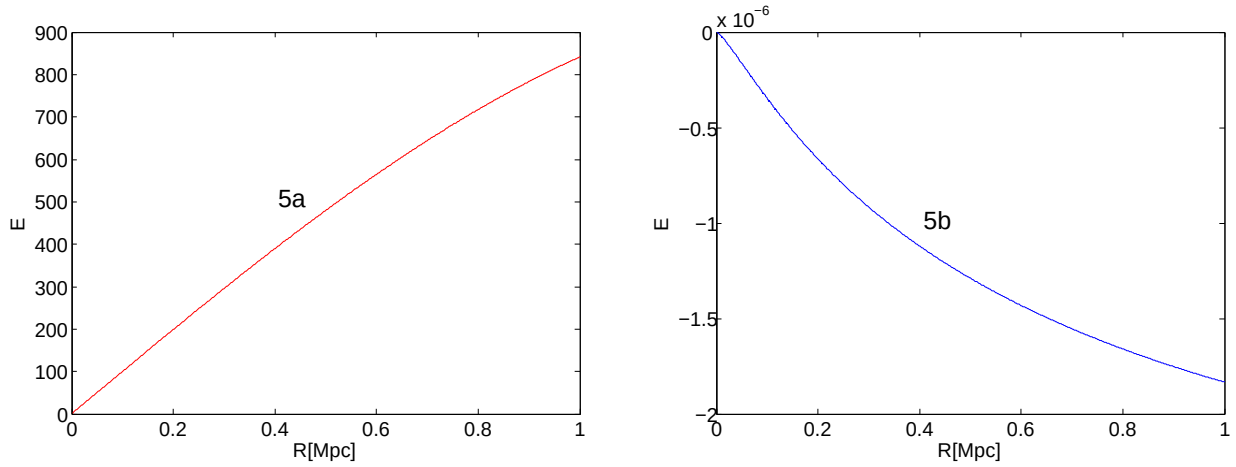

Figure 5.3: E for Models 5a and 5b

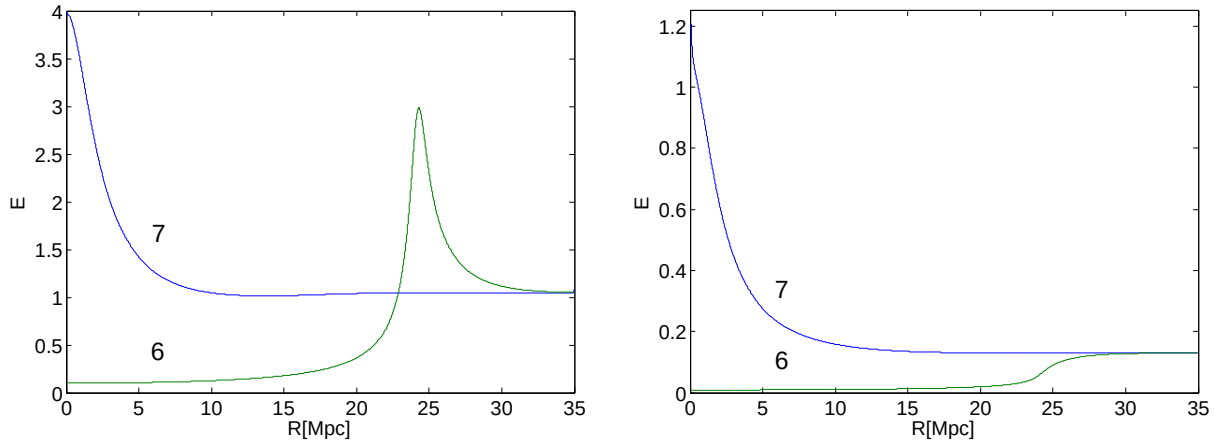

(a) The current density profile

(b) The volume deceleration parameter

Figure 5.4: Models 6 and 7 - models of cosmic structure

Models 6 and 7

Models 6 and 7 specified in the appendix of [14] do not yield the plots given in the paper. Conversations with Bolejko (reference conversation) helped deduce the correct models as given in appendix A of this report.

Model 6 is a toy void and model 7 is a toy supercluster. Figure (5.4*a*) shows the density profile of models 6 and 7 at the current epoch and figure (5.4*b*) plots the volume deceleration parameter as a function of the areal distance at the current epoch t_0. Both models are observed to have a positive volume deceleration parameter, and as stated in [14], the volume deceleration can be made negative with a change in the model, but as with the other models this yields a very large $t_B(r)$ and so an unrealistic age of the Universe.

The method used for finding q^{vol} for these models was much more involved than earlier ones,

requiring an evolution from distributions at the time of last scattering to the current time, see Appendix B for more details.

Model 8

This model was chosen as an example of what can happen when the volume deceleration parameter is negative. First let it be noted that figure (5.5*b*) is different from figure 5, right panel in [14]. Bolejko agrees that a mistake must have been made in their calculation or in writing the paper itself (reference). It is not shown very well in this plot, but in the limit as $R \to 0$ $q^{vol} \to 2$. This is in contrast to the figure in [14] where $q^{vol} \approx 0$. We have a volume deceleration for small R, but as we include more data for larger R, it becomes negative at $R \approx 6.667$ Mpc. A calculation of the bang time as a function of r yields figure 5.6. This levels off to a value of $t_B \approx 11 \times 10^9$ yr leaving an unrealistically small age of the Universe.

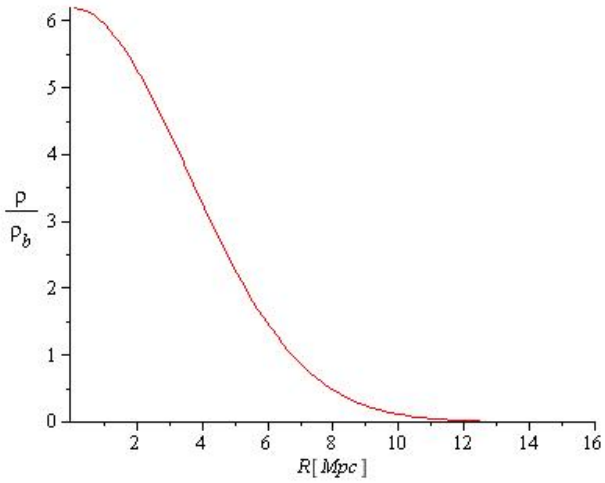

(a) Current density distribution

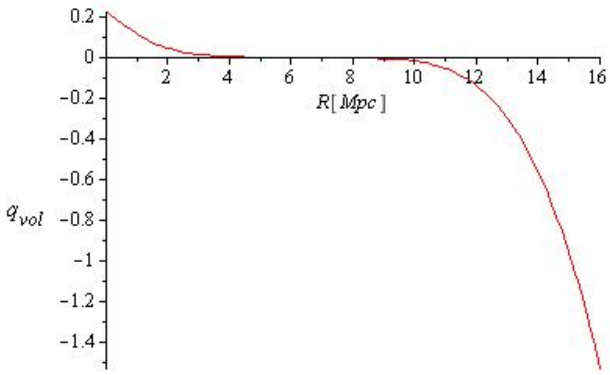

(b) The volume deceleration parameter

Figure 5.5: Model 8

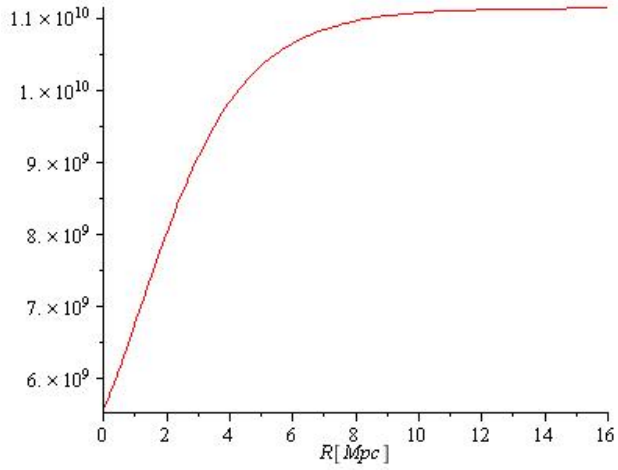

Figure 5.6: The bang time for model 8

Chapter 6

Conclusion

This project followed the analysis of Bolejko and Andersson [14]. The Lemaître–Tolman model and Buchert averaging scheme were studied in order to compare the deceleration parameter derived from luminosity distance and the deceleration parameter of the Buchert scheme. Within the Buchert scheme we showed an important commutation rule which states that in the presence of general inhomogeneities, averaging after evolving is not the same as evolving after averaging. Bolejko and Andersson's analysis was "motivated by recent results showing that there are models which despite Λ being zero, the average expansion rate is accelerating" [14] i.e., $\ddot{a} > 0$ from equation (2.27). These models opened the possibility that backreaction and averaging effects can explain away the problem of dark energy. Buchert and Weigard believe this to be possible and explore backreaction in [28] whereas there are others including Wiltshire who take alternative stances. Wiltshire explores an extension of the strong equivalence principle leading to dark energy being a misidentification of gravitational energy gradients and variance in clock rates [29].

We have reanalysed the two deceleration parameters within four Lemaître-Tolman models (models 1-4) which have a good fit to supernova 1a observations. The results obtained mean that the two deceleration parameters are not *directly* related in agreement with [14], but this does not rule out the possibility of any relationship. (*something about possible possibilities*).

This shows that our search for models to fit supernova 1a data with $\Lambda = 0$ need not be restricted to cases with $q^{vol} < 0$. In fact, within the models analysed here with $q^{vol} < 0$, including those for cosmic structure, the ages of the Universe was found to be unrealistic.

We have also corrected some errors in [14] including model 6 and 7 specifications and the q^{vol} curve for model 8.

Bibliography

[1] A. Friedman. Über die Krümmung des Raumes. *Zeitschrift für Physik A Hadrons and Nuclei*, 10(1):377–386, 1922.

[2] A. Friedmann. Über die Möglichkeit einer Welt mit konstanter negativer Krümmung des Raumes. *Zeitschrift für Physik A Hadrons and Nuclei*, 21(1):326–332, 1924.

[3] Richard Kessler et al. First-year Sloan Digital Sky Survey-II (SDSS-II) Supernova Results: Hubble Diagram and Cosmological Parameters. *Astrophys. J. Suppl.*, 185:32–84, 2009.

[4] E. Komatsu et al. Seven-Year Wilkinson Microwave Anisotropy Probe (WMAP) Observations: Cosmological Interpretation. 2010.

[5] Peter Anninos. Computational cosmology: From the earliy universe to the large scaler structure. 2001', eprint =.

[6] Kari Enqvist. Lemaitre-Tolman-Bondi model and accelerating expansion. *Gen. Rel. Grav.*, 40:451–466, 2008.

[7] J. Richard Gott, III et al. A Map of the Universe. *Astrophys. J.*, 624:463, 2005.

[8] C. Armendariz-Picon, Viatcheslav F. Mukhanov, and Paul J. Steinhardt. A dynamical solution to the problem of a small cosmological constant and late-time cosmic acceleration. *Phys. Rev. Lett.*, 85:4438–4441, 2000.

[9] Thomas Buchert. On average properties of inhomogeneous fluids in general relativity. I: Dust cosmologies. *Gen. Rel. Grav.*, 32:105–125, 2000.

[10] Aseem Paranjape and T.P. Singh. The possibility of cosmic acceleration via spatial averaging in Lemaître-Tolman-Bondi models. *Classical Quantum Gravity*, 23(23):6955–6969, 2006.

[11] Tomohiro Kai, Hiroshi Kozaki, Ken-ichi Nakao, Yasusada Nambu, and Chul-Moon Yoo. Can inhomogeneities accelerate the cosmic volume expansion? *Prog. Theor. Phys.*, 117(2):229–240, 2007.

[12] Yasusada Nambu and Masayuki Tanimoto. Accelerating universe via spatial averaging. 2005.

[13] Roberto A. Sussman. On the spatial volume averaging in Lemaitre-Tolman-Bondi dust models. 1. Back reaction, spatial curvature and binding energy. 2008.

[14] Krzysztof Bolejko and Lars Andersson. Apparent and average acceleration of the Universe. *JCAP*.

[15] Richard L. Arnowitt, Stanley Deser, and Charles W. Misner. The dynamics of general relativity. 1962.

[16] S.M. Carroll. *Spacetime and geometry. An introduction to general relativity.* 2004.

[17] B. DeWitt(eds) R. K. Sachs, in C. DeWitt. *Relativity, Groups and Topology.* Gordon and Breach, 1964. pp. 523 - 564.

[18] S. Räsänen. Backreaction in the Lemaître–Tolman–Bondi model. *Journal of Cosmology and Astroparticle Physics*, 2004:010, 2004.

[19] G. Lemaitre. *Ann. Soc. Sci. Bruxelles*, A53(51), 1933.

[20] R.C. Tolman. *Proc. Natl. Acad. Sci.*, 20(169), 1934.

[21] H. Bondi. *Mon. Not. R. Astron. Soc.*, 107(410), 1947.

[22] K. Enqvist and T. Mattsson. The effect of inhomogeneous expansion on the supernova observations. *Journal of Cosmology and Astroparticle Physics*, 2007:019, 2007.

[23] Maria Mattsson and Teppo Mattsson. On the role of shear in cosmological averaging. 2010.

[24] A. Krasiński and C. Hellaby. Structure formation in the Lemaitre-Tolman model. *Physical Review D*, 65(2):23501, 2001.

[25] Kari Enqvist and Teppo Mattsson. The effect of inhomogeneous expansion on the supernova observations. *JCAP*, 0702:019, 2007.

[26] Adam G. Riess et al. New Hubble Space Telescope Discoveries of Type Ia Supernovae at $z > 1$: Narrowing Constraints on the Early Behavior of Dark Energy. *Astrophys. J.*, 659:98–121, 2007.

[27] Julio F. Navarro, Carlos S. Frenk, and Simon D. M. White. The Structure of Cold Dark Matter Halos. *Astrophys. J.*, 462:563–575, 1996.

[28] Alexander Wiegand and Thomas Buchert. Multiscale cosmology and structure-emerging Dark Energy: A plausibility analysis. *Phys. Rev.*, D82:023523, 2010.

[29] David L. Wiltshire. From time to timescape - Einstein's unfinished revolution. *Int. J. Mod. Phys.*, D18:2121–2134, 2009.

Appendix A

Model Specification

The models considered in [14] follow, added for completeness. Note that this appendix is based on that given in [14] with many errors removed and a few additional notes where needed.

As stated in Chapter 3, we require two functions and a choice of gauge to uniquely specify the solution to a Lemaître-Tolman model.

(i) Models 1 and 2
The chosen gauge is $r = R(r, t_0)$. These models are specified by a present day density distribution, $\rho(r, t_0)$, and the big bang time function $t_B(r)$. We have:

$$\rho(r, t_0) = \rho_b \left[1 + \delta_\rho - \delta_\rho \exp\left(-\frac{r^2}{\sigma^2}\right)\right]$$

where $\rho_b = \Omega_m(3H_0^2)/(8\pi G)$ – the Friedmann background density (the same in models, 1-5 and 8) , $\Omega_m = 0.27$, $H_0 = 70$ km s^{-1} Mpc^{-1} (also the same for models 1-5 and 8). For model 1: $\delta_b = 1.9$ and $\sigma = 0.9$ Gpc. For model 2: $\delta_b = 1.5$ and $\sigma = 0.5$Gpc respectively. Our big bang time is chosen to occur simultaneously at every point, thus $t_B(r) = 0$. Functions $M(r)$ and $E(r)$ are calculated using equations (3.3) and (3.4) respectively. Alternatively $E(r)$ can be calculated using the algorithm in Appendix B, as has been done in this project. The time instants are calculated using the formula:

$$t(z) = \frac{1}{H_0}\int_z^\infty \frac{dx}{(1+x)\sqrt{(\Omega_m(1+x)^3 + (1-\Omega_m)(1+x)^2)}}$$

The time of last scattering, t_{LS}, is set to take place when $z = 1089$ and current instant is t_0, occurring when $z = 0$, which have been calculated using the above integral to be $t_{LS} = 4.98 \times 10^5$y and $t_0 = 11.4421 \times 10^9$y.

(ii) Models 3 and 4
Again, the chosen gauge is $r = R(r, t_0)$. These models are specified by the current expansion rate and the assumption that $\rho(r, t_0) = \rho_b$. We have:

$$H_T(t_0, r) = \frac{\dot{R}}{R} = H_0 \left[1 - \delta_H + \delta_H \exp\left(-\frac{r^2}{\sigma^2}\right)\right],$$

For model 3: $\delta_H = 9.6/H_0$ and $\sigma = 0.6$Gpc. For model 4: $\delta_H = 12/H_0$ and $\sigma = 1.2$Gpc. $M(r)$ can be found via equation (3.3) and used with (3.2) and H_T to find $E(r)$.

(iii) Model 5a
Again, choose $r = R(r, t_0)$. This model is defined by the density distributions at present and last scattering. At present we have:

$$\rho(r, t_0) = \rho_b \frac{\delta}{\left(\frac{r}{r_s}\right)\left(1 + \frac{r}{r_s}\right)^2}$$

with $\delta = 28170$ and $r_s = 191$kpc. The singularity at the origin can be overcome by matching this profile with a singularity free profile, as $f(r) = -ar^2 + b$. The two functions are matched at $r = r_*$ when $\rho(r_*, t_0) = f(r_*)$ and $\frac{d}{dr}\rho(r, t_0)|_{r=r_*} = \frac{d}{dr}f(r)|_{r=r_*}$. The density profile at last scattering is assumed to be homogeneous; thus integration of (3.2) yields the areal distance at last scattering:

$$R(r, t_{LS}) = \left(\frac{6M(r)}{\kappa\rho(r, t_{LS})c^2}\right)$$

$M(r)$ can be found via (3.2) evaluated at $t = t_0$. $E(r)$ can be found using an algorithm analogous to that found in Appendix B, explained in [24].

(iv) Model 5*b*
As in models 1-4 we set $r = R(r, t_0)$. The model is defined by $\rho(r, t_0)$ in 5*a* and $E(r)$ is specified by:

$$E(r) = 10^3 \sin(r\text{Mpc}^{-1})$$

(v) Models 6 and 7
The gauge chosen here is $r = R(r, t_{LS})$. Both models are defined with $t_B(r) = 0$ and the density distribution as last scattering:

$$\rho(r, t_{LS}) = \rho_b \left(1 - \delta\exp\left[-\left(\frac{lr}{k}\right)^2\right] + \gamma\exp\left[-\left(\frac{lr - c}{d}\right)^2\right]\right)$$

where $l = 1\text{kpc}^{-1}$. For model 6: $\delta = 1.2 \times 10^{-3}$, $\gamma = 14.62 \times 10^{-4}$, $k = 10$, $c = 18$, and $d = 6$. Model 7: $\delta = -2 \times 10^{-3}$, $\gamma = -8.03 \times 10^{-5}$, $k = 5$, $c = 12$ and $d = 5$. It is noted that we have $\rho_b = (1 + z)^3\Omega_m(3H_0^2)/(8\pi G)$ with $H_0 = 65$ km s^{-1} Mpc, $z = 1089$ and $t_{LS} = 5.359 \times 10^5$ yr, $t_0 = 12.3223389 \times 10^9$ yr. The bang time of each model is defined to be $t_B(r) = 0$. $M(r)$ can be calculated from (3.3) and $E(r)$ using (3.4) or as shown in Appendix B.

(vi) Model 8
As in models 1-5 we set $r = R(r, t_0)$. The density distribution is given by:

$$\rho(r, t_0) = 6.2\rho_b\exp[-4 \times 10^{-8}(lr)^2],$$

and the function E(r):

$$E(r) = \left(\frac{H_0}{c}r\right)^2 \exp(10^{-3}lr),$$

with ρ_b, H_0, t_0 as in models 1-5.

Appendix B

Methods

This algorithm was used to solve for $E(r)$ and can be found in [24], and was used in models 1, 2, 6 and 7. A similar algorithm can be made for model $5a$, see [24] for more details.

1. Assume t_i ($= t_0$ for models 1 and 2, $= t_{LS}$ for models 6 and 7) and $R(r, t_i) = r$ and evaluate $M(r)$ using model specifications and equation (3.2)
2. Calculate $t_x = \frac{\sqrt{2}}{3c} \frac{R^{3/2}}{M^{1/2}}$
3. Consider three cases:
   - $t_i = t_x \implies E = 0$
   - $t_i < t_x \implies E > 0$. To find E one needs to solve:
   $$0 = ct_i - \frac{M}{(2E)^{3/2}} \left[\sqrt{(1 + 2ER/M)^2 - 1} - \operatorname{arcosh}(1 + 2ER/M) \right]$$
   - $t_y > t_i > t_x \implies E < 0$ (so-called 'still expanding') where $t_y = \frac{\pi}{2^{3/2}c} \frac{R^{3/2}}{M^{1/2}}$. To find E one needs to solve:
   $$0 = ct_i - \frac{M}{(-2E)^{3/2}} \left[\arccos(1 + 2ER/M) - \sqrt{1 - (1 + 2ER/M)^2} \right]$$

We note that this leaves the case $t_i > t_x$ and $t_i > t_y$. In [24] this case is also dealt with, but none of our models involve this case which is why it is omitted.

In some of the models looked at, density at the time of last scattering, t_{LS}, is given and we must evolve our density profile up to the current time, t_0, in order to calculate q^{vol}. Assuming we already know $M(r)$ and $E(r)$, this is done by rearranging equation (3.2) to give:

$$\dot{R}(r, t) = \pm \sqrt{2E(r) + \frac{2M(r)}{R(r, t)}} \tag{B.1}$$

where the $\pm$ is dependent on whether the model is "expanding" or "collapsing" for a given region [1]. All models looked at in this report are "expanding" apart from model $5a$, and so

[1] See (**??**) for more details about when a model is expanding or contracting.

for all models apart from $5a$ we use the + branch. We then solve this differential equation for $R(r,t)$ using a numerical integration package. Now the density at t_0 can be found by rearranging (3.3) for $\rho(r,t)$ and evaluating at $t = t_0$.